Research Article

Structure Preserving Numerical Analysis of Reaction-Diffusion Models

Nauman Ahmed (ID),[1,2] **Muhammad Aziz-ur Rehman,**[2] **Waleed Adel** (ID),[3,4] **Fahd Jarad** (ID),[5,6] **Mubasher Ali,**[7] **Muhammad Rafiq,**[8] **and Ali Akgül** (ID)[9]

[1]*Department of Mathematics and Statistics, The University of Lahore, Lahore, Pakistan*
[2]*Department of Mathematics, University of Management and Technology, Lahore, Pakistan*
[3]*Department of Mathematics and Engineering Physics, Faculty of Engineering, Mansoura University, Mansoura, Egypt*
[4]*Université Française d'Egypte, Ismailia Desert Road, El Shorouk, Cairo, Egypt*
[5]*Department of Mathematics, Çankaya University, 06790 Etimesgut, Ankara, Turkey*
[6]*Department of Medical Research, China Medical University, Taichung 40402, Taiwan*
[7]*School of Engineering and Digital Arts, University of Kent, Canterbury Kent, UK*
[8]*Department of Mathematics, Faculty of Sciences, University of Central Punjab, Lahore, Pakistan*
[9]*Siirt University, Art and Science Faculty, Department of Mathematics, TR-56100, Siirt, Turkey*

Correspondence should be addressed to Fahd Jarad; fahd@cankaya.edu.tr

In this paper, we examine two structure preserving numerical finite difference methods for solving the various reaction-diffusion models in one dimension, appearing in chemistry and biology. These are the finite difference methods in splitting environment, namely, operator splitting nonstandard finite difference (OS-NSFD) methods that effectively deal with nonlinearity in the models and computationally efficient. Positivity of both the proposed splitting methods is proved mathematically and verified with the simulations. A comparison is made between proposed OS-NSFD methods and well-known classical operator splitting finite difference (OS-FD) methods, which demonstrates the advantages of proposed methods. Furthermore, we applied proposed NSFD splitting methods on several numerical examples to validate all the attributes of the proposed numerical designs.

1. Introduction

A system of differential equations represents the dynamics of real-life phenomenon. These systems can be applied in the field of physics, chemistry, fluid dynamics, engineering, economics, biological sciences etc. Initially, only temporal systems were used to observe the dynamics of different situations. But, for studying the most general behaviors of such systems, we can include the additional quantities such as advection and diffusion in the systems of differential equations. These systems depict the generic situations of the temporal and spatial models [1–3]. Reaction-diffusion equations are considered as one of the most important equations that are used in the modeling of chemical and

biological systems. Certain phenomena such as population densities, concentration of chemical substance, and pressure of fluid are described by the state variables of such systems. Therefore, the positivity of state variables is an important requirement for the discrete scheme and should not produce nonphysical oscillations and negative solutions. There is not much work in the literature for positivity preserving and chaos-free numerical methods for chemical reaction models. In this study, we have designed two operator splitting positivity preserving and chaos-free numerical schemes for various reaction diffusion models arising in chemistry and biology.

In this paper, three different models of reaction diffusion equations in one-space dimension are considered for the

study. The main aim of this work is to find the numerical solutions of these models with reliable numerical techniques. These proposed techniques preserve the structure of continuous systems in one dimension.

First of all, among these important models, we consider the Brusselator system that is used in describing the simulations of nonlinear oscillations in chemical reaction-diffusion processes [4–7]. The importance of oscillation in a biochemical system is very significant and was first introduced by Turning et al. [8]. They showed that when some phenomena are considered with diffusion term, a stable spatial pattern is obtained. Also, this system appears in a wide variety of models, such as ozone formation during oxygen atoms collision and enzymatic reactions. The reaction diffusion Brusselator system contains a couple of variables which intervene with reactions, and this process produces chemicals whose concentrations are then controlled. This model has been revealed as the trimolecular model.

Due to the importance of such models, many powerful and efficient techniques have been proposed for solving this system. Such models with nonlinear evolution terms are very hard to solve with the aid of analytical methods. Therefore, numerical methods are needed while dealing with such models. For example, Mittal et al. [9–11] investigated the solution of the one-dimensional Brusselator system using the differential quadrature technique. The behaviour of one-dimensional version of the Brusselator system is studied in [12] with the aid of collocation method based on the radial bases functions. A B-spline approach with a modification was introduced by Jiwari and Yuan in [13] for the Brusselator system with one and two dimensions. Also, a three dimensional form of this system was first solved in [14] using the modified B-spline differential quadrature method. Lin et al. [15] studied the inhomogeneous Brusselator model with cross diffusion process by using a finite volume element approximation and performed the stability analysis for the method and addressed the formation of turning patterns. A new exact solution for this system was driven using the exp-function method in [16]. For more details about the methods for solving the Brusselator model, see [17–20] and references therein.

The Brusselator reaction-diffusion model in one dimension is given as follows:

$$\frac{\partial \psi_1}{\partial t} = \varepsilon_{\psi_1} \frac{\partial^2 \psi_1}{\partial x^2} + \vartheta_2 - (\vartheta_1 + 1)\psi_1 + (\psi_1)^2 \psi_2, \tag{1}$$

$$\frac{\partial \psi_2}{\partial t} = \varepsilon_{\psi_2} \frac{\partial^2 \psi_2}{\partial x^2} + \vartheta_1 \psi_1 - (\psi_1)^2 \psi_2, \tag{2}$$

with initial conditions

$$\psi_1(x, 0) = \alpha(x), \quad 0 \leq x \leq L, \tag{3}$$

$$\psi_2(x, 0) = \beta(x), \quad 0 \leq x \leq L, \tag{4}$$

and homogeneous Neumann boundary conditions

$$\frac{\partial \psi_1(0, t)}{\partial x} = \frac{\partial \psi_1(L, t)}{\partial x} = 0, \quad t > 0, \tag{5}$$

$$\frac{\partial \psi_2(0, t)}{\partial x} = \frac{\partial \psi_2(L, t)}{\partial x} = 0, \quad t > 0. \tag{6}$$

As discussed earlier that $\psi_1(x, t)$ and $\psi_2(x, t)$ are the concentrations of the chemical substances or species, ϑ_1 and ϑ_2 represent the concentrations' constants that appear in the reaction process, and ε_{ψ_1} and ε_{ψ_2} are the diffusion constants. The equilibrium point of systems (1) and (2) is $(\psi_1^*, \psi_2^*) = (\vartheta_2, \vartheta_1/\vartheta_2)$. The point (ψ_1^*, ψ_2^*) is stable if $1 - \vartheta_1 + \vartheta_2^2 \geq 0$ and unstable if $1 - \vartheta_1 + \vartheta_2^2 < 0$. The solution to the system represented by equations (1) and (2) describes the positivity criteria as ψ_1 and ψ_2 are the concentrations of the two species [21]. Therefore, negative values of the solution of this model are meaningless. The numerical technique applied to find the solution of system by the coupled equation in (1) and (2) must preserve the positivity.

The finite-difference technique is an important tool to solve the nonlinear model involving differential equations. Because finding the analytical solution of such models is not an easy task. Therefore, various authors used finite-difference numerical schemes to solve several mathematical models involving ordinary differential equations or partial differential equations [22–28].

The nonstandard finite difference method (NSFD) is a powerful technique for solving different type of nonlinear continuous models which was first presented by Mickens back in 1993 [29]. Over the years, this method proved that it can treat continuous dynamical models that should preserve positivity property. For example, Ahmed et al. [30] adapt the NSFD scheme for solving different types of such models including the SEIR reaction diffusion model. Detailed discussion regarding NSFD and positivity preserving techniques can be found in [31–37].

The paper is organized as follows: in Section 2, four numerical techniques are presented for solving the Brusselator model. In Section 3, the stability and accuracy of the presented methods are introduced. Section 4 is devoted for illustrating the positivity of the purposed schemes. The applications of various reaction-diffusion systems along with the comparison of the four presented methods are presented in Section 5. Lastly, Section 6 provides conclusion for the study.

2. Numerical Techniques

In this section, we will introduce four techniques for solving systems (1)and(2) subjected to condition (3) and homogeneous Neumann boundary conditions. These numerical methods can be divided into two classical methods named as forward and backward operator splitting methods and two nonclassical methods named as explicit and implicit OS-NSFD methods. Each of these method has its own pros and cons. These methods are explained as follows.

2.1. Forward Euler Operator Splitting Method. In the current section, the first method is introduced which is a splitting method based on a finite difference scheme. The splitting

techniques are computationally efficient and handle the complexity and nonlinearity of the differential equations. The main idea of these methods is to split the main equation into two-equation system. The nonlinear reaction steps are described as

$$\frac{1}{2}\frac{\partial \psi_1}{\partial t} = \vartheta_2 - (\vartheta_1 + 1)\psi_1 + (\psi_1)^2\psi_2,$$
$$\frac{1}{2}\frac{\partial \psi_2}{\partial t} = \vartheta_1\psi_1 - (\psi_1)^2\psi_2. \tag{7}$$

Here, ϑ_1 and ϑ_2 represent the concentrations's constants that appears in the reaction process. These last mentioned equations are then utilized for the solution of the linear part of the diffusion equation at the first half step for time as

$$\frac{1}{2}\frac{\partial \psi_1}{\partial t} = \varepsilon_{\psi_1}\frac{\partial^2 \psi_1}{\partial x^2},$$
$$\frac{1}{2}\frac{\partial \psi_2}{\partial t} = \varepsilon_{\psi_2}\frac{\partial^2 \psi_2}{\partial x^2}, \tag{8}$$

that are used for the second equal time step.

For the finite difference approximations, divide $[0, L] \times [0, T]$ into $M \times N$ with $\omega = L/M$ and $\kappa = T/N$.

Grid points are $x_i = i\omega, i = 0, 1, 2, \ldots, M$, $t_n = n\kappa, n = 0, 1, 2, \ldots, N$, and $\psi_{1_i}^n$ and $\psi_{2_i}^n$ describe the difference approximations of $\psi_1(i\omega, n\kappa)$ and $\psi_2(i\omega, n\kappa)$, respectively. Then, the proposed scheme is used to solve these equations in the form:

$$\overline{\psi_{1i}}^{n+(1/2)} = \psi_{1_i}^n + \kappa\vartheta_2 - \kappa(\vartheta_1 + 1)\psi_{1_i}^n + \kappa(\psi_{1_i}^n)^2 u_{2_i}^n,$$
$$\overline{\psi_{2i}}^{n+(1/2)} = \psi_{2_i}^n + \kappa\vartheta_1\psi_{1_i}^n - \kappa(\psi_{1_i}^n)^2\psi_{2_i}^n, \tag{9}$$

where $\overline{\psi}_{1_i}^{n+(1/2)}$ and $\overline{\psi}_{2_i}^{n+(1/2)}$ demonstrate the concentrations at the first equal step of time and $\psi_1(t_{n+(1/2)}) = \psi_1(t_n + (1/2)\omega)$ and $\psi_2(t_{n+(1/2)}) = \psi_2(t_n + (1/2)\omega)$. At the next step of time, the form is

$$\psi_{1_i}^{n+1} = \overline{\psi}_{1_i}^{n+(1/2)} + \lambda_1\left(\overline{\psi}_{1_{i-1}}^{n+(1/2)} - 2\overline{\psi}_{1_i}^{n+(1/2)} + \overline{\psi}_{1_{i+1}}^{n+(1/2)}\right), \tag{10}$$

$$\psi_{2_i}^{n+1} = \overline{\psi}_{2_i}^{n+(1/2)} + \lambda_2\left(\overline{\psi}_{2_{i-1}}^{n+(1/2)} - 2\overline{\psi}_{2_i}^{n+(1/2)} + \overline{\psi}_{2_{i+1}}^{n+(1/2)}\right). \tag{11}$$

The boundary condition (5) is incorporated in (10) and (11) by using central difference approximation as

$$\frac{\psi_{1_{i+1}}^n - \psi_{1_{i-1}}^n}{2\omega} = 0, \quad \text{which implies that}$$
$$\psi_{1_1}^n = \psi_{1_{-1}}^n,$$
$$\psi_{1_{M+1}}^n = \psi_{1_{M-1}}^n, \tag{12}$$

with initial conditions as

$$\psi_{1_i}^0 = \alpha(x_i),$$
$$\psi_{2_i}^0 = \beta(x_i). \tag{13}$$

2.2. Backward Euler Operator Splitting Method.

Now, in this section, we will implement the backward Euler OS-FD technique to solve the Brusselator system. The procedure for the first half step of time is given as

$$\overline{\psi_{1i}}^{n+(1/2)} = \psi_{1_i}^n + \kappa\vartheta_2 - \kappa(\vartheta_1 + 1)\psi_{1_i}^n + \kappa(\psi_{1_i}^n)^2\psi_{2_i}^n, \tag{14}$$

$$\overline{\psi_{2i}}^{n+(1/2)} = \psi_{2_i}^n + \kappa\vartheta_1\psi_{1_i}^n - \kappa(\psi_{1_i}^n)^2\psi_{2_i}^n, \tag{15}$$

which is identical to the last scheme. At the next equal step of time, the final form for the above mentioned scheme is

$$-\lambda_1\psi_{1_{i-1}}^{n+1} + (1 + 2\lambda_1)\psi_{1_i}^{n+1} - \lambda_1\psi_{1_{i-1}}^{n+1} = \overline{\psi}_{1_i}^{n+(1/2)}, \tag{16}$$

$$-\lambda_2\psi_{2_{i-1}}^{n+1} + (1 + 2\lambda_2)\psi_{2_i}^{n+1} - \lambda_2\psi_{2_{i-1}}^{n+1} = \overline{\psi}_{2_i}^{n+(1/2)}. \tag{17}$$

The boundary condition (5) is incorporated in (16) and (17) by using central difference approximation as

$$\frac{\psi_{1_{i+1}}^n - \psi_{1_{i-1}}^n}{2\omega} = 0, \quad \text{which implies that}$$
$$\psi_{1_1}^n = \psi_{1_{-1}}^n,$$
$$\psi_{1_{M+1}}^n = \psi_{1_{M-1}}^n, \tag{18}$$

with initial conditions as,

$$\psi_{1_i}^0 = \alpha(x_i),$$
$$\psi_{2_i}^0 = \beta(x_i). \tag{19}$$

2.3. Operator Splitting Nonstandard Explicit Finite Difference Method.

Here, we turn our attention to construct a novel method based on a nonstandard finite difference and an operator splitting method named as (OS-NSFD) explicit scheme. For this, we apply the rules defined by Mickens [29] and the designed OS-NSFD technique at the first half time step is described as

$$\overline{\psi}_{1_i}^{n+(1/2)} = \frac{\psi_{1_i}^n + \kappa\vartheta_2 + \kappa(\psi_{1_i}^n)^2\psi_{2_i}^n}{1 + \kappa(\vartheta_1 + 1)}, \tag{20}$$

$$\overline{\psi}_{2_i}^{n+(1/2)} = \frac{\psi_{2_i}^n + \kappa\vartheta_1\psi_{1_i}^n}{1 + \kappa(\psi_{1_i}^n)^2}. \tag{21}$$

For the second equal time step, the strategy for aforementioned technique is

$$\psi_{1_i}^{n+1} = (1 - 2\lambda_1)\overline{\psi}_{1_i}^{n+(1/2)} + \lambda_1\left(\overline{\psi}_{1_{i-1}}^{n+(1/2)} + \overline{\psi}_{1_{i+1}}^{n+(1/2)}\right), \tag{22}$$

$$\psi_{2_i}^{n+1} = (1 - 2\lambda_2)\overline{\psi}_{2_i}^{n+(1/2)} + \lambda_2\left(\overline{\psi}_{2_{i-1}}^{n+(1/2)} + \overline{\psi}_{2_{i+1}}^{n+(1/2)}\right). \tag{23}$$

The boundary condition (5) is incorporated in (22) and (23) by using central difference approximation as

$$\frac{\psi_{1_{i+1}}^n - \psi_{1_{i-1}}^n}{2\omega} = 0, \quad \text{which implies that}$$

$$\psi_{1_1}^n = \psi_{1_{-1}}^n, \tag{24}$$

$$\psi_{1_{M+1}}^n = \psi_{1_{M-1}}^n,$$

with initial conditions as

$$\begin{aligned}\psi_{1_i}^0 &= \alpha(x_i),\\ \psi_{2_i}^0 &= \beta(x_i).\end{aligned} \tag{25}$$

2.4. Operator Splitting Nonstandard Implicit Finite Difference Method. This section is devoted for the second proposed novel scheme named as OS-NSFD implicit scheme. The designed OS-NSFD implicit technique at the first half step of time is

$$\overline{\psi}_{1_i}^{n+(1/2)} = \frac{\psi_{1_i}^n + \kappa\vartheta_2 + \kappa\left(\psi_{1_i}^n\right)^2 \psi_{2_i}^n}{1 + \kappa(\vartheta_1 + 1)}, \tag{26}$$

$$\overline{\psi}_{2_i}^{n+(1/2)} = \frac{\psi_{2_i}^n + \kappa\vartheta_1 \psi_{1_i}^n}{1 + \kappa\left(\psi_{1_i}^n\right)^2}. \tag{27}$$

For the next step, the final form of current technique is

$$-\lambda_1\psi_{1_{i-1}}^{n+1} + (1 + 2\lambda_1)\psi_{1_i}^{n+1} - \lambda_1\psi_{1_{i-1}}^{n+1} = \overline{\psi}_{1_i}^{n+(1/2)}, \tag{28}$$

$$-\lambda_2\psi_{2_{i-1}}^{n+1} + (1 + 2\lambda_2)\psi_{2_i}^{n+1} - \lambda_2\psi_{2_{i-1}}^{n+1} = \overline{\psi}_{2_i}^{n+(1/2)}. \tag{29}$$

The boundary condition (5) is incorporated in (28) and (29) by using central difference approximation as

$$\frac{\psi_{1_{i+1}}^n - \psi_{1_{i-1}}^n}{2\omega} = 0, \quad \text{which implies that}$$

$$\psi_{1_1}^n = \psi_{1_{-1}}^n, \tag{30}$$

$$\psi_{1_{M+1}}^n = \psi_{1_{M-1}}^n,$$

with initial conditions as

$$\begin{aligned}\psi_{1_i}^0 &= \alpha(x_i),\\ \psi_{2_i}^0 &= \beta(x_i).\end{aligned} \tag{31}$$

In all above numerical schemes, the value of $\lambda_1 = \varepsilon_{\psi_1}(\kappa/\omega^2)$ and $\lambda_2 = \varepsilon_{\psi_2}(\kappa/\omega^2)$.

3. Stability and Consistency of Underlying Techniques

In this section, the stability along with the consistency of the solution for all the above operator splitting methods is investigated. In all of these methods, the time derivative has an accuracy of $O(\kappa)$ when solved exactly for the reaction step.

The diffusion step, in the same way, has an $O(\omega^2)$ accuracy, and the accumulative accuracy for all the techniques is first order and second order in time and space, respectively. The reaction steps are proven to be unconditionally stable for all the methods illustrated above when solving in an exact way [38,39]. In forward Euler OS-FD and explicit NSFD techniques represented in equations (22) and (23), the stability region is

$$\lambda_i \leq \frac{1}{2}, \quad (i = 1, 2, 3). \tag{32}$$

In addition, for the Euler OS-FD and implicit NSFD methods, the stability for the diffusion process is found to be stable without any conditions.

Next, we will study the positivity of the solution by considering all of the above schemes.

4. Positivity of the Proposed Schemes

This section is concerned with the validation of positivity of the designed NSFD explicit and implicit techniques. The following theorem verifies that the proposed explicit technique retains the positivity of the solution.

Theorem 1. *The solution of the proposed explicit techniques in the given formulas (20), (21), (26), and (27) at the reaction step with the assumptions of nonnegative initial conditions, i.e.,*

$$\psi_{1_i}^n \geq 0, \psi_{2_i}^n \geq 0 \Rightarrow \psi_{1_i}^{n+(1/2)} \geq 0, \psi_{2_i}^{n+(1/2)} \geq 0. \tag{33}$$

Theorem 1 verifies that the property of positivity of the solution is preserved by the proposed OS-NSFD schemes at the reaction step.

Remark 1. A positive solution is achieved by using the explicit NSFD method represented in equations (22) and (23) if

$$1 - 2\lambda_i \geq 0, \quad i = 1, 2. \tag{34}$$

From the above expression, it is clear that

$$\lambda_i \leq \frac{1}{2}, \quad (i = 1, 2), \tag{35}$$

which is the same stability condition as (32) of the OS-NSFD explicit method. This proves that the OS-NSFD explicit method can preserve positivity within its stability region.

We, then utilize the M-matrix theory [40] which helps in proving the positivity property for the proposed OS-NSFD implicit method (28)-(29).

Theorem 2. *For any $\omega > 0$ and $\kappa > 0$, systems (28) and (29) are positive, i.e., $\psi_1^n > 0$ and $\psi_2^n > 0$ for all $n = 0, 1, 2\ldots$.*

Proof. Systems (28) and (29) can be written as

$$\Theta \psi_1^{n+1} = \psi_1^n, \tag{36}$$

$$\Phi \psi_2^{n+1} = \psi_2^n. \tag{37}$$

In the above equations, Θ and Φ are the square matrices as follows:

$$\Theta = \begin{pmatrix} \Theta_3 & \Theta_1 & 0 & \cdots & \cdots & \cdots & \cdots & 0 \\ \Theta_2 & \Theta_3 & \Theta_2 & \ddots & & & & \vdots \\ 0 & \Theta_2 & \Theta_3 & \Theta_2 & \ddots & & & \vdots \\ \vdots & \ddots & \ddots & \ddots & \ddots & \ddots & & \vdots \\ \vdots & & \ddots & \ddots & \ddots & \ddots & \ddots & \vdots \\ \vdots & & & \ddots & \Theta_2 & \Theta_3 & \Theta_2 & 0 \\ \vdots & & & & \ddots & \Theta_2 & \Theta_3 & \Theta_2 \\ 0 & \cdots & \cdots & \cdots & \cdots & 0 & \Theta_1 & \Theta_3 \end{pmatrix}, \tag{38}$$

$$\Phi = \begin{pmatrix} \Phi_3 & \Phi_1 & 0 & \cdots & \cdots & \cdots & \cdots & 0 \\ \Phi_2 & \Phi_3 & \Phi_2 & \ddots & & & & \vdots \\ 0 & \Phi_2 & \Phi_3 & \Phi_2 & \ddots & & & \vdots \\ \vdots & \ddots & \ddots & \ddots & \ddots & \ddots & & \vdots \\ \vdots & & \ddots & \ddots & \ddots & \ddots & \ddots & \vdots \\ \vdots & & & \ddots & \Phi_2 & \Phi_3 & \Phi_2 & 0 \\ \vdots & & & & \ddots & \Phi_2 & \Phi_3 & \Phi_2 \\ 0 & \cdots & \cdots & \cdots & \cdots & 0 & \Phi_1 & \Phi_3 \end{pmatrix}. \tag{39}$$

The off-diagonal entries of Θ are $\Theta_1 = -2\lambda_1$ and $\Theta_2 = -\lambda_1$, and diagonal entries are $\Theta_3 = 1 + 2\lambda_1$. The off-diagonal entries of Φ are $\Phi_1 = -2\lambda_1$ and $\Phi_2 = -\lambda_1$, and diagonal entries are $\Phi_3 = 1 + 2\lambda_2$. Thus, Θ, and Φ are M-matrices. Therefore, expressions (36) and (37) can be written as

$$\psi_1^{n+1} = \Theta^{-1}\psi_1^n, \tag{40}$$

$$\psi_2^{n+1} = \Phi^{-1}\psi_2^n. \tag{41}$$

If we consider that $\psi_1^n > 0$ and $\psi_2^n > 0$, then we get that $\psi_1^{n+1} > 0$ and $\psi_2^{n+1} > 0$, with the aid of the property of M-matrix and Theorem 1. So, the result is then proved by induction. From this theorem, we conclude that the implicit OS-NSFD preserves the property of positivity unconditionally. □ □

5. Application

To support our claims regarding the proposed OS-NSFD techniques, we will implement these schemes to several reaction diffusion models along with the famous Brusselator model.

5.1. Brusselator Model. For the application of the proposed and classical methods under study, we chose the following numerical test. The graphical behaviour of the solution for each of the proposed four methods are demonstrated

through the following figures for solving systems (1) and (2). As discussed above, systems (1) and (2) have a positive solution and converge toward the equilibrium point if the condition $1 - \vartheta_1 + \vartheta_2^2 \geq 0$ is satisfied and unstable if $1 - \vartheta_1 + \vartheta_2^2 < 0$.

First, Figures 1 and 2 demonstrates the simulated results for the first method which is the forward Euler OS-FD technique at various step sizes. It can be noticed from these figures that this method gives nonconsistent data with systems (1) and (2). This proves that this method gives negative values of the concentrations which is meaningless. Also, the solution diverge from the equilibrium point which contradict with the physical behavior of the solution.

The second method is tested on the same example which is the backward Euler OS-FD method with the same value of parameters as in the first method for the sake of comparison. The behavior of the solution is illustrated in Figures 3 and 4. These figures show that this method, like the first method, fails to preserve the positivity of the solution and also gives divergence.

The graphical behaviour of the state variables show that the forward Euler and backward Euler OS-FD method are not the reliable techniques to solve the nonlinear auto-catalytic chemical reaction model. As they provide us with the negative solutions for the small step sizes.

Due to the failure of the two abovementioned methods, the NSFD methods are presented to overcome this issue. Figures 5 and 6 show the graphs of the solution using the explicit OS-NSFD method. For the sake of comparison with the other methods, we use the same values of the parameters which are used in the previous two methods and took the value of ϑ_1 and ϑ_2 such that $1 - \vartheta_1 + \vartheta_2^2 \geq 0$. From these figures, unlike the other methods, we observe that this method preserves the positivity and all the important properties of the glycolysis continuous model and converges toward the equilibrium point.

The graphs in Figures 7 and 8 demonstrate the concentrations by using the implicit OS-NSFD method. This behavior is also shown to be consistent with the explicit OS-NSFD method. This method like the previous method also preserves positivity and chaos-free properties and converges towards the equilibrium point which is stable under the condition $1 - \vartheta_1 + \vartheta_2^2 \geq 0 > 0$.

Now, the simulations by using both designed OS-NSFD techniques are given by considering the values of parameters ϑ_1 and ϑ_2 so that $1 - \vartheta_1 + \vartheta_2^2 > 0$.

As mentioned before, the stability of the Brusselator system is preserved with the condition $1 - \vartheta_1 + \vartheta_2^2 > 0$. Figures 9 and 10 prove this fact that the two new presented OS-NSFD methods are consistent with the continuous model when the stability condition holds and are inconsistent when $1 - \vartheta_1 + \vartheta_2^2 < 0$. Figures 9 and 10 reflect the inconsistent behavior when the stability criterion does not hold, while the other while the other parameters and step sizes and kept fixed. This fact has been proven that stability criteria is very important in the stability analysis.

Now, we consider $T = 1$ and $M = 100$. Figure 11 depicts log-log graphs of the error versus the computational time. We presented the four schemes, and the graphs correspond
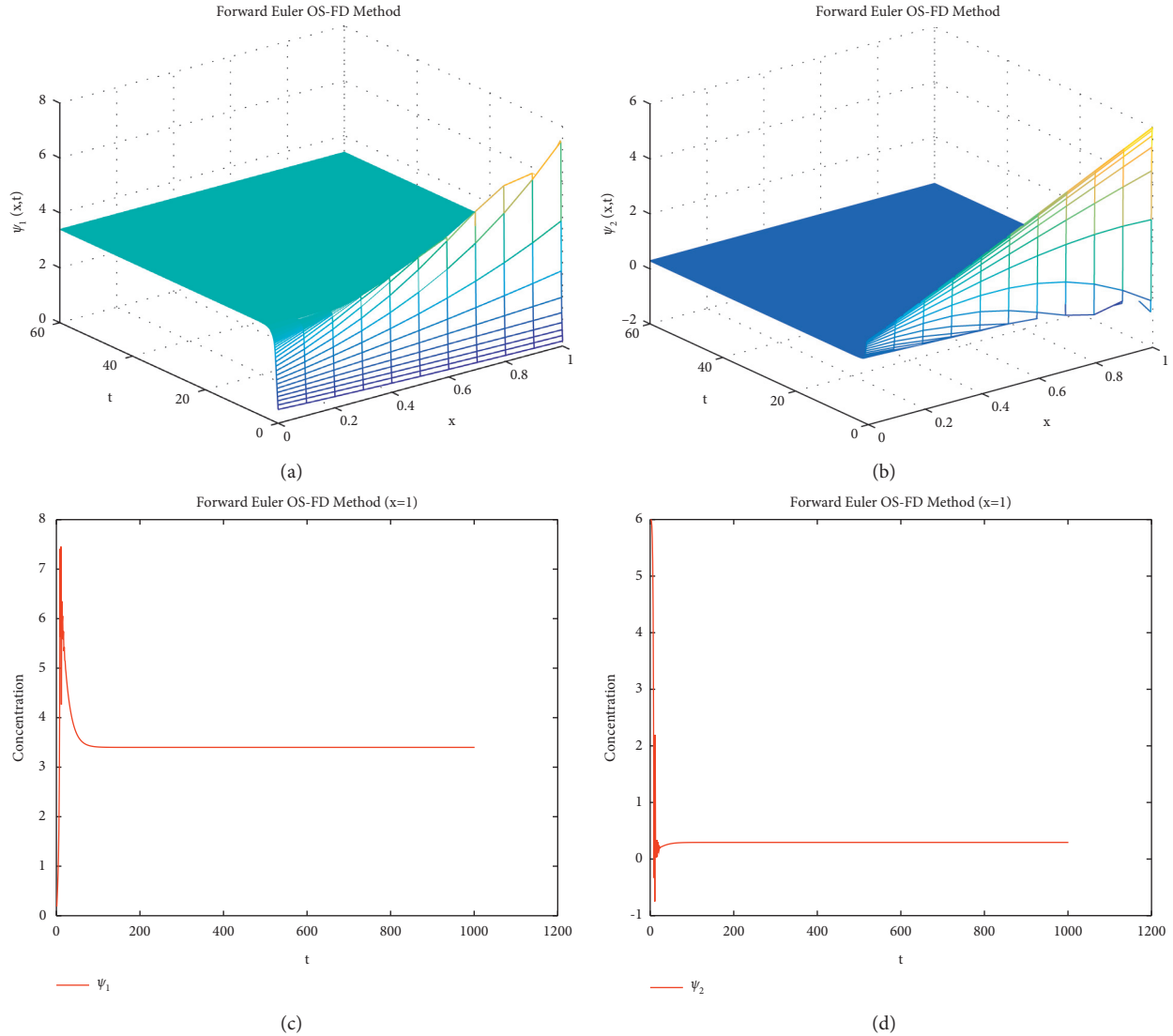
(a)

(b)

(c)

(d)

FIGURE 1: Mesh graphs and plot graphs of ψ_1 and ψ_2 (concentration profile) using forward Euler OS-FD method at $\kappa = 0.1, \vartheta_1 = 1, \vartheta_2 = 3.4, \lambda_1 = \lambda_2 = 0.0006,$ and $\varepsilon_{\psi_1} = \varepsilon_{\psi_1} = 10^{-4}$. (a) Solution graph of ψ_1. (b) Solution graph of ψ_2. (c) Plot graph of ψ_1. (d) Plot graph of ψ_2.

to the solutions when we estimate the concentration profiles ψ_1 and ψ_2 of the Brusselator system. The result demonstrates that the OS-NSFD explicit and implicit schemes are approximately as efficient as forward Euler OS-FD and backward Euler OS-FD schemes. Obviously, the former technique stands out in terms of its capability to preserve the structure of the relevant solutions of the Brusselator model under investigation. It is worth pointing out that the approximation to the exact solution was obtained using $N = 20000$.

Finally, four numerical methods are used to solve the underlying model, namely, the forward Euler operator splitting method, backward Euler operator splitting method, nonstandard finite difference explicit operator splitting method, and nonstandard finite difference implicit operator splitting method. The extensively used numerical Euler

methods (backward and forward) are used to solve the underlying models. The obtained solutions are analyzed and compared with the newly developed methods. The failure of the classical methods motivated us to develop new numerical methods. The new techniques are structure-preserving and reliable numerical methods that give positive and bounded solutions. The computed solutions converge towards the exact steady-state. So, the numerical analysis demonstrates that the NSFD methods are the reliable tool to solve the nonlinear models.

5.2. Susceptible-Infected-Recovered Epidemic Model. For the second application, we consider nonlinear reaction-diffusion system of infectious disease dynamics. The system is known as susceptible-infected-recovered (SIR) epidemic [41],
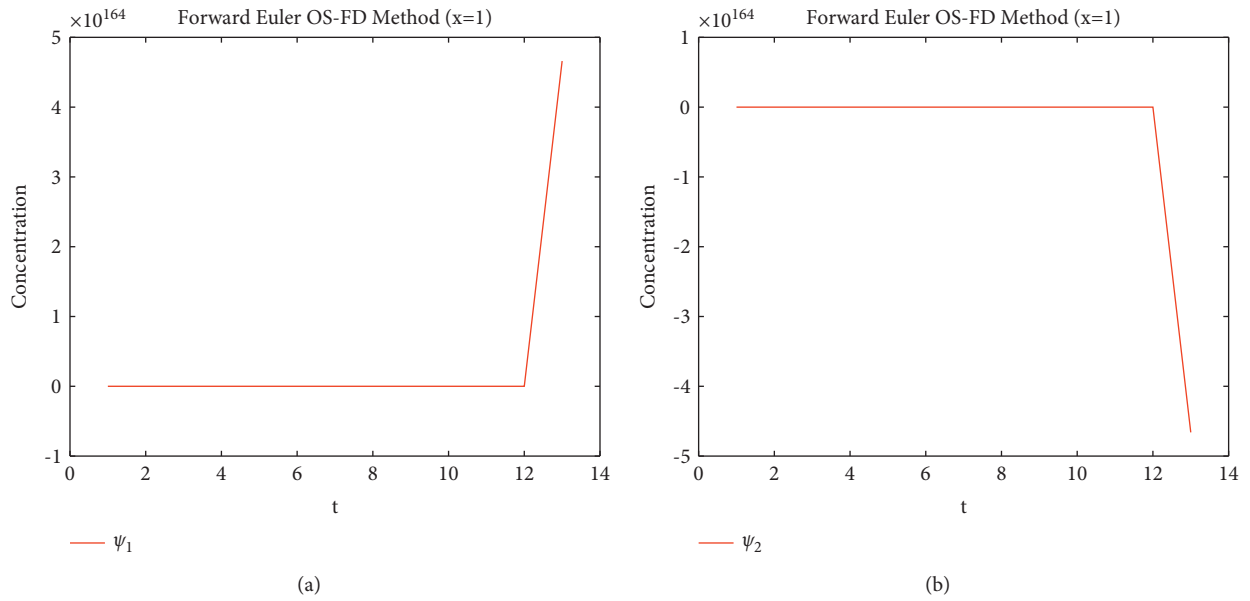
(a)

(b)

FIGURE 2: Plot graphs of ψ_1 and ψ_2 implementing the forward Euler OS-FD technique at $\kappa = 0.1, \vartheta_1 = 1, \vartheta_2 = 3.4, \lambda_1 = \lambda_2 = 0.001$, and $\varepsilon_{\psi_1} = \varepsilon_{\psi_1} = 10^{-4}$. (a) Plot graph of ψ_1. (b) Plot graph of ψ_2.
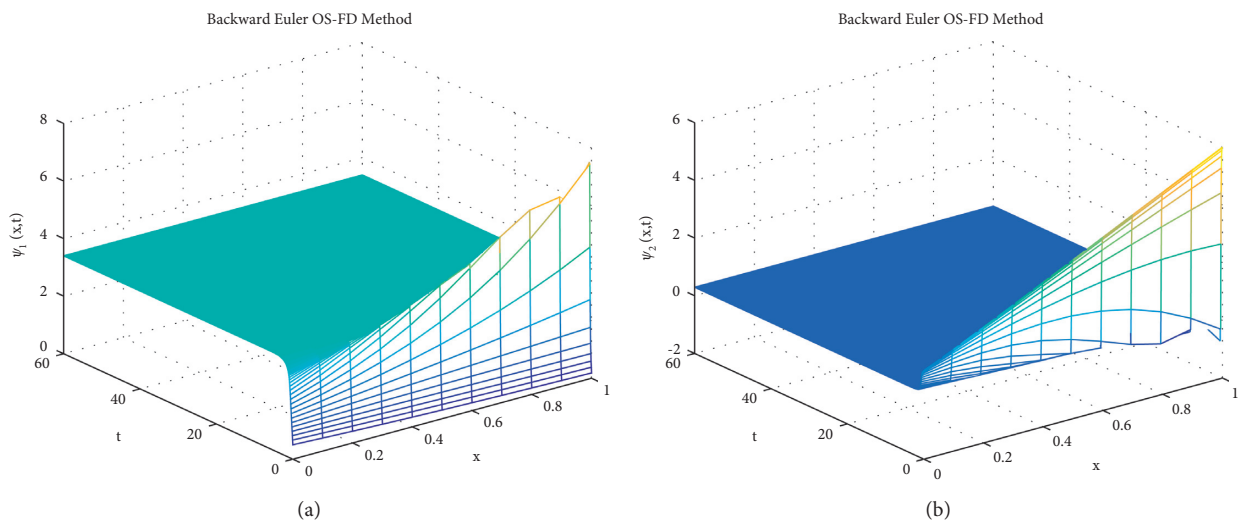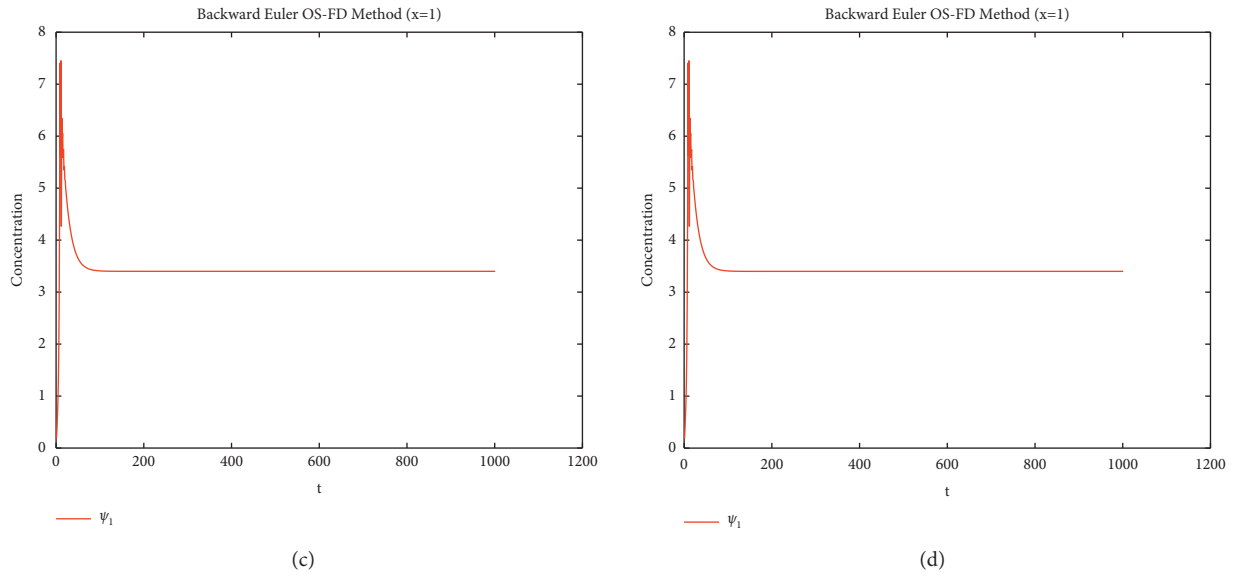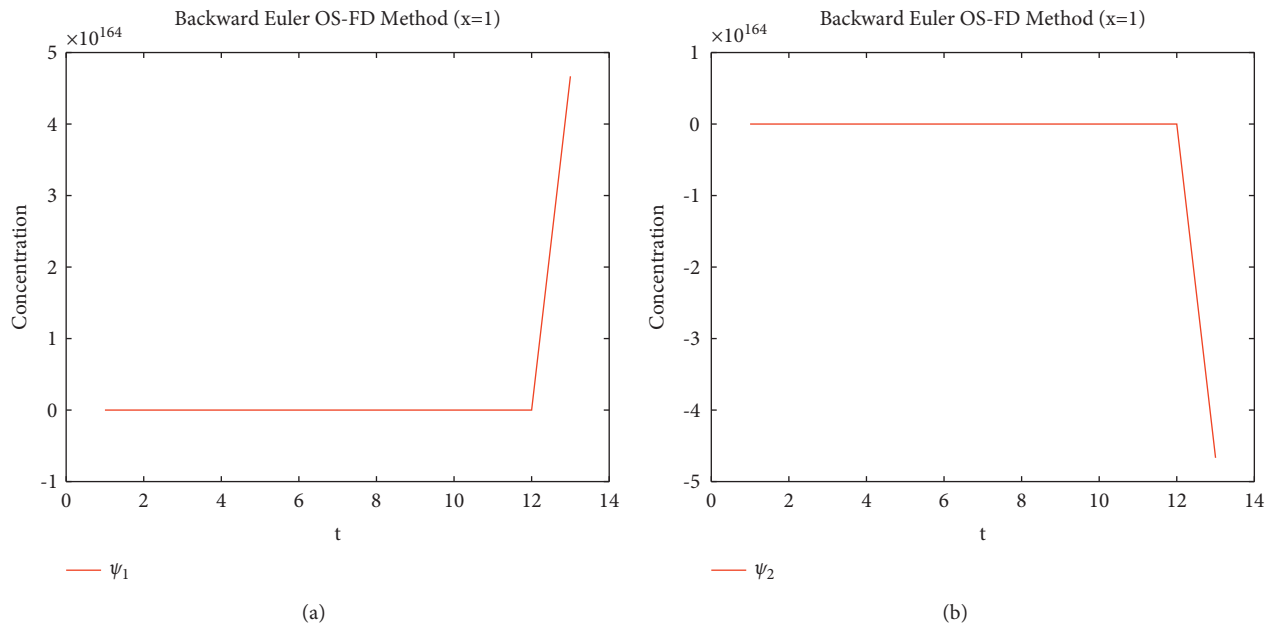

(a)

(b)

FIGURE 3: Continued.

(c)

(d)

FIGURE 3: Solution graphs and plot graphs of ψ_1 and ψ_2 implementing backward Euler OS-FD technique at $\kappa = 0.1, \vartheta_1 = 1, \vartheta_2 = 3.4, \lambda_1 = \lambda_2 = 0.0006$, and $\varepsilon_{\psi_1} = \varepsilon_{\psi_1} = 10^{-4}$. (a) Solution graph of ψ_1. (b) Solution graph of ψ_2. (c) Plot graph of ψ_1. (d) Plot graph of ψ_2.

(a)

(b)

FIGURE 4: Plot graphs of ψ_1 and ψ_2 implementing the backward Euler OS-FD method at $\kappa = 0.01, \vartheta_1 = 1, \vartheta_2 = 3.4, \lambda_1 = \lambda_2 = 0.001$, and $\varepsilon_{\psi_1} = \varepsilon_{\psi_1} = 10^{-4}$. (a) Plot graph of ψ_1. (b) Plot graph of ψ_2.
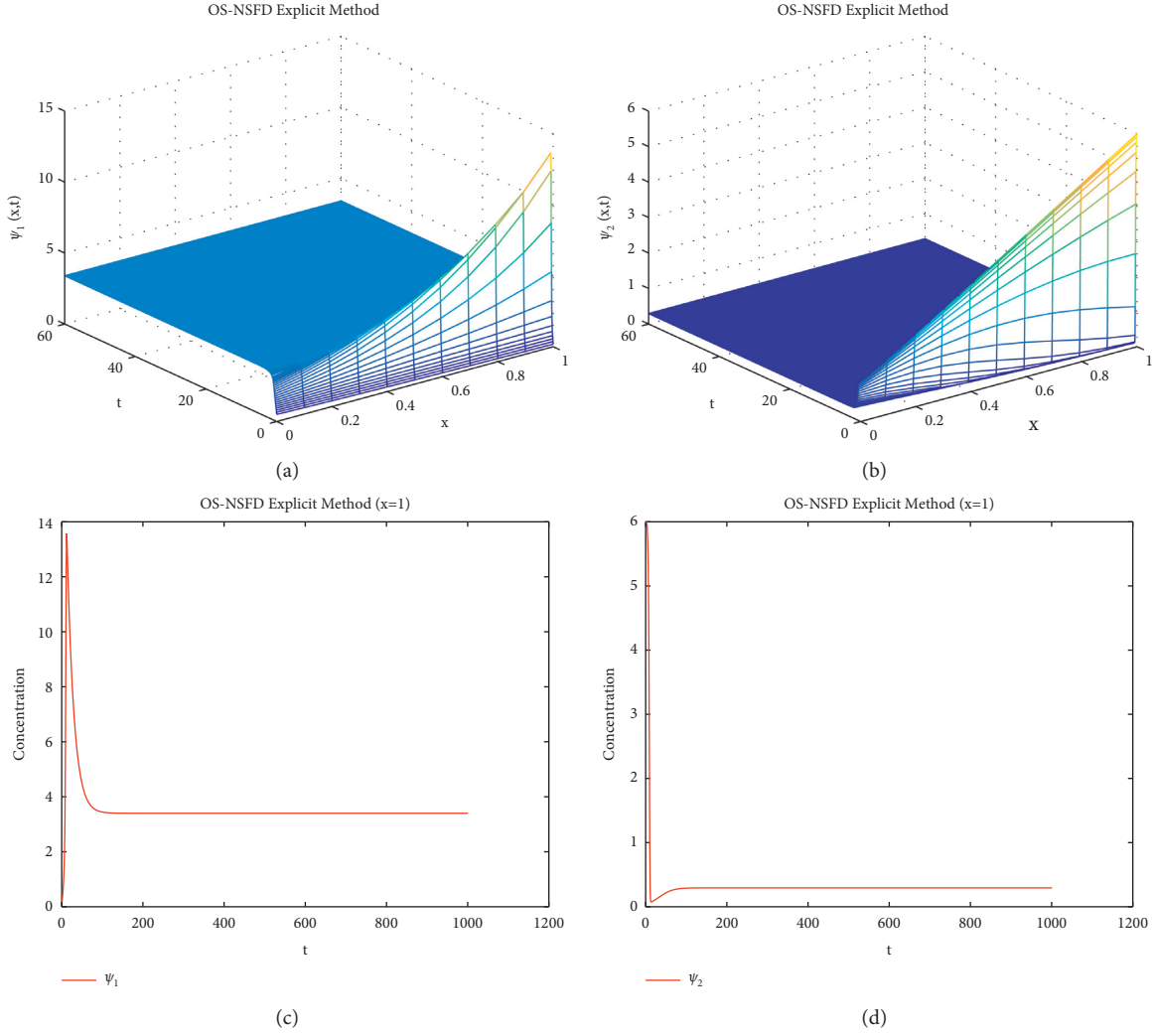
FIGURE 5: Mesh graphs and plot graphs of ψ_1 and ψ_2 implementing NSFD explicit splitting method at $\kappa = 0.1, \vartheta_1 = 1, \vartheta_2 = 3.4, \lambda_1 = \lambda_2 = 0.0006$, and $\varepsilon_{\psi_1} = \varepsilon_{\psi_1} = 10^{-4}$. (a) Mesh graph of ψ_1. (b) Mesh graph of ψ_2. (c) Plot graph of ψ_1. (d) Plot graph of ψ_2.

$$\frac{\partial \psi_1}{\partial t} = \varepsilon_{\psi_1} \frac{\partial^2 \psi_1}{\partial x^2} + \vartheta_1 N - \vartheta_1 \psi_1 - \vartheta_3 \psi_1 \psi_2, \tag{42}$$

$$\frac{\partial \psi_2}{\partial t} = \varepsilon_{\psi_2} \frac{\partial^2 \psi_2}{\partial x^2} - (\vartheta_1 + \vartheta_2)\psi_2 + \vartheta_3 \psi_1 \psi_2, \tag{43}$$

with initial conditions

$$\psi_1(x,0) = \begin{cases} 325000x, & 0 \le x \le \dfrac{1}{2}, \\\\ 325000(1-x), & \dfrac{1}{2} \le x \le 1, \end{cases}$$
$$\psi_2(x,0) = \begin{cases} 7500x, & 0 \le x \le \dfrac{1}{2}, \\\\ 7500(1-x), & \dfrac{1}{2} \le x \le 1, \end{cases} \tag{44}$$

and homogeneous Neumann boundary conditions. In systems (42) and (43), $\psi_1 = \psi_1(x,t)$ and $\psi_2 = \psi_2(x,t)$ are susceptible and infected population densities. ϑ_1 is the parameter which represents natural birth and death rate. ϑ_2 indicates the rate of recovery from infected to recovered class. The transmission coefficient from susceptibility to disease is denoted by ϑ_3.

The epidemic systems (42) and (43) have two stable fixed points, disease-free point (DFP) and endemic point (EP). DFP is the point when disease eradicates from the population. The DFP of systems (42)and(43) $\epsilon_0 = (N, 0)$. The EP is the point when disease persists in the population. The EP of systems (42)and(43) is $\epsilon_* = (\psi_{1*}, \psi_{2*})$, where $\psi_{1*} = (\vartheta_1 + \vartheta_2)/\vartheta_3$ and $\vartheta_{2*} = (\vartheta_1 N/(\vartheta_1 + \vartheta_2)) - (\vartheta_1/\vartheta_3)$.

The basic reproductive number of the epidemic system (42)and(43) is $\mathcal{B}_0 = N\vartheta_3/\vartheta_1 + \vartheta_2$ when $d_{\psi_i} = 0, i = 1, 2$. $\mathcal{B}_0$ is very important quantity which decides whether disease is e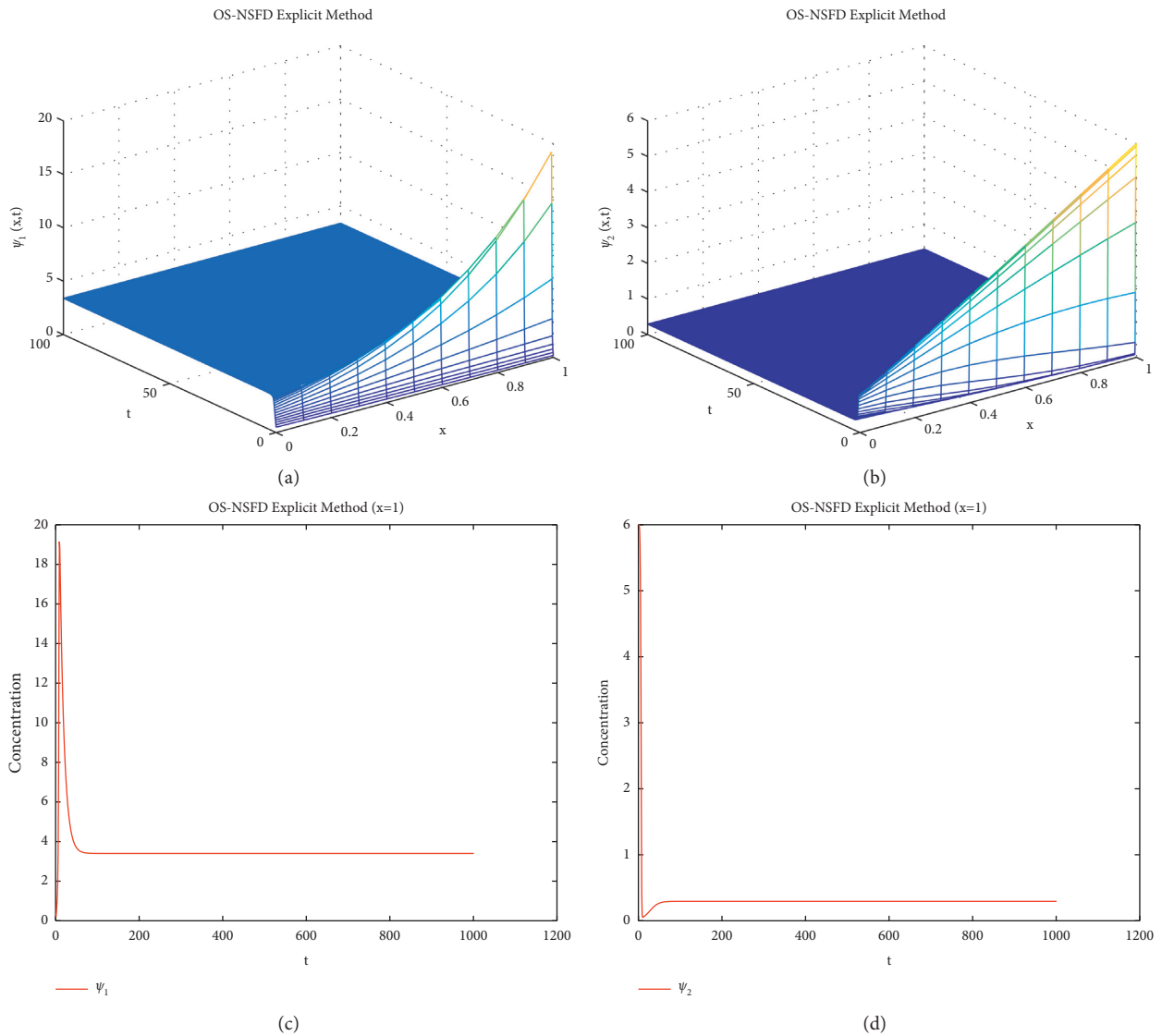radicated or persisted. If $\mathcal{B}_0 < 1$, then disease will wipe out, and the disease is present if $\mathcal{B}_0 > 1$.

(a)

(b)

(c)

(d)

FIGURE 6: Mesh and plot graphs of ψ_1 and ψ_2 implementing NSFD explicit splitting technique at $\kappa = 0.1, \vartheta_1 = 1, \vartheta_2 = 3.4, \lambda_1 = \lambda_2 = 0.001,$ and $\varepsilon_{\psi_1} = \varepsilon_{\psi_1} = 10^{-4}$. (a) Mesh graph of ψ_1. (b) Mesh graph of ψ_2. (c) Plot graph of ψ_1. (d) Plot graph of ψ_2.
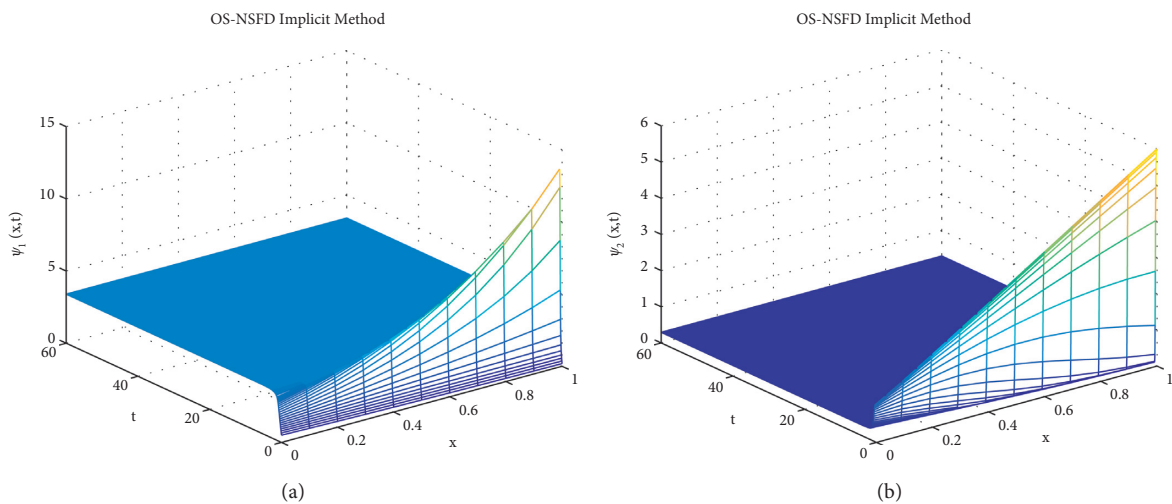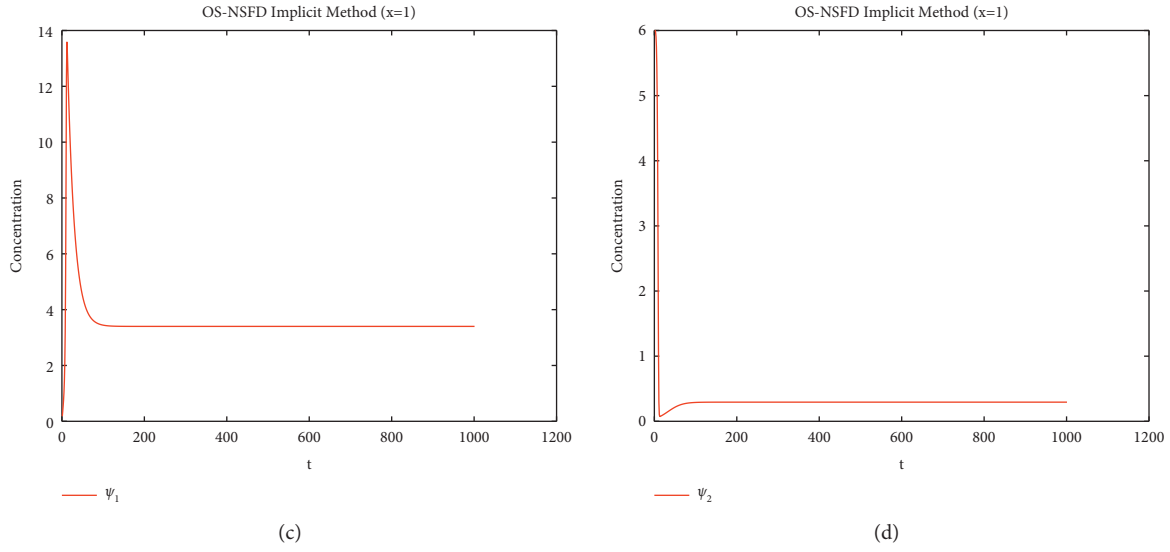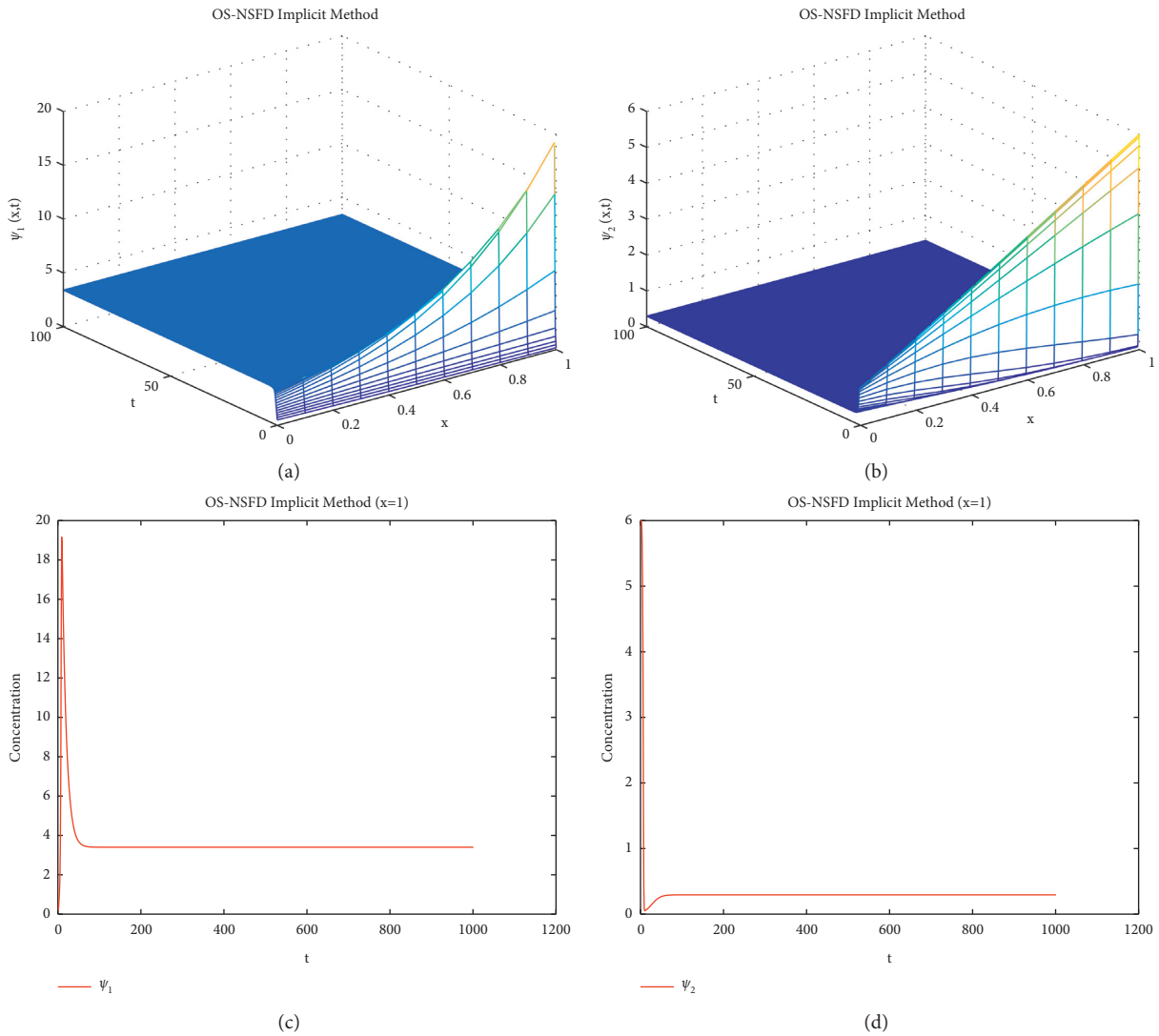

(a)

(b)

FIGURE 7: Continued.

FIGURE 7: Mesh graphs and plot graphs of ψ_1 and ψ_2 implementing NSFD implicit splitting technique at $\kappa = 0.1, \vartheta_1 = 1, \vartheta_2 = 3.4, \lambda_1 = \lambda_2 = 0.0006,$ and $\varepsilon_{\psi_1} = \varepsilon_{\psi_1} = 10^{-4}$. (a) Mesh graph of ψ_1. (b) Mesh graph of ψ_2. (c) Plot graph of ψ_1. (d) Plot graph of ψ_2.

FIGURE 8: Mesh and plot graphs of ψ_1 and ψ_2 implementing NSFD implicit splitting method at $\kappa = 0.1, \vartheta_1 = 1, \vartheta_2 = 3.4, \lambda_1 = \lambda_2 = 0.001,$ and $\varepsilon_{\psi_1} = \varepsilon_{\psi_1} = 10^{-4}$. (a) Solution graph of ψ_1. (b) Solution graph of ψ_2. (c) Plot graph of ψ_1. (d) Plot graph of ψ_2.
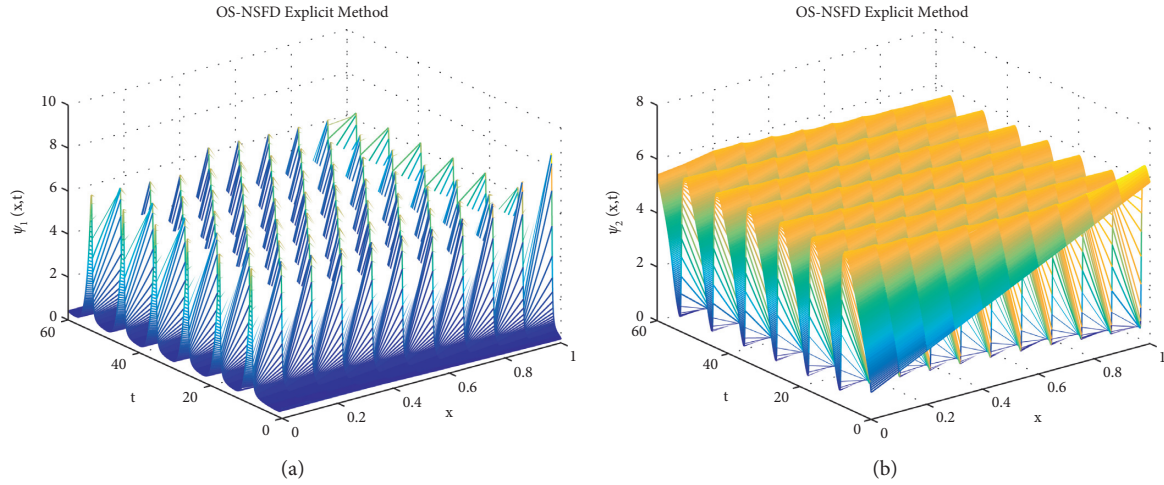
(a)

(b)

FIGURE 9: Solution graphs of ψ_1 and ψ_2 implementing NSFD explicit splitting technique at $\kappa = 0.1, \vartheta_1 = 3.4, \vartheta_2 = 1, \lambda_1 = \lambda_2 = 0.0006$, and $\varepsilon_{\psi_1} = \varepsilon_{\psi_1} = 10^{-4}$. (a) Solution graph of ψ_1. (b) Solution graph of ψ_2.
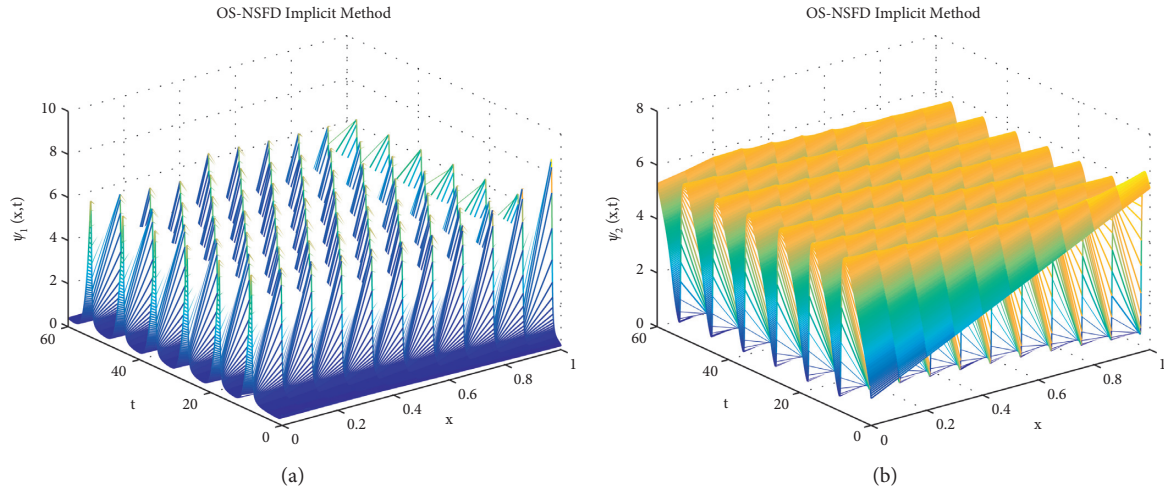

(a)

(b)

FIGURE 10: Solution graphs of ψ_1 and ψ_2 implementing NSFD implicit splitting method at $\kappa = 0.1, \vartheta_1 = 1, \vartheta_2 = 3.4, \lambda_1 = \lambda_2 = 0.0006$, and $\varepsilon_{\psi_1} = \varepsilon_{\psi_1} = 10^{-4}$. (a) Solution graph of ψ_1. (b) Solution graph of ψ_2.

In the above experiment, we use the following numerical values of parameters involved in the above system. $N = 3 \times 10^{-05}, \vartheta_1 = 0.04, \vartheta_2 = 24$, and $\varepsilon_{\psi_1} = \varepsilon_{\psi_2} = 0.01$. First, we depict the simulations of OS-NSFD explicit and implicit schemes at DFP. For the DFP, we take the value $\vartheta_3 = 9.2 \times 10^{-07}$ so that $\mathscr{B}_0 < 1$.

The simulations in the Figures 12 and 13 describe that the proposed splitting methods show positive solution as well as preserves the stability of fixed point DFP $\epsilon_0 = (N, 0) = (3 \times 10^{-05})$ under the condition $\mathscr{B}_0 < 1$. This shows that the designed NSFD splitting techniques do not show the contrived chaos.

Also, the graphs for susceptible and infected individuals reflect the positive and bounded solutions. It is notable that

those graphs converge towards the exact fixed points for the step sizes, and other parameter values are mentioned above.

Next, we present the simulations of OS-NSFD explicit and implicit schemes at EP. For the EP, we use the value $\vartheta_3 = 1.4 \times 10^{-03}$ so that $\mathscr{B}_0 > 1$.

As we have taken the values of parameters so that $\mathscr{B}_0 > 1$. This implicates that SIR epidemic model converges toward EP $\epsilon_* = (\psi_{1*}, \psi_{2*})$. The simulation executed in Figures 14 and 15 illustrate the positive behavior and convergence to the EP $\epsilon_* = (\psi_{1*}, \psi_{2*})$ of NSFD explicit and implicit splitting schemes. In the light of the above discussion, it can be concluded that OS-NSFD explicit and implicit methods are reliable numerical methods for the solution of reaction diffusion models. Because these methods confine all the
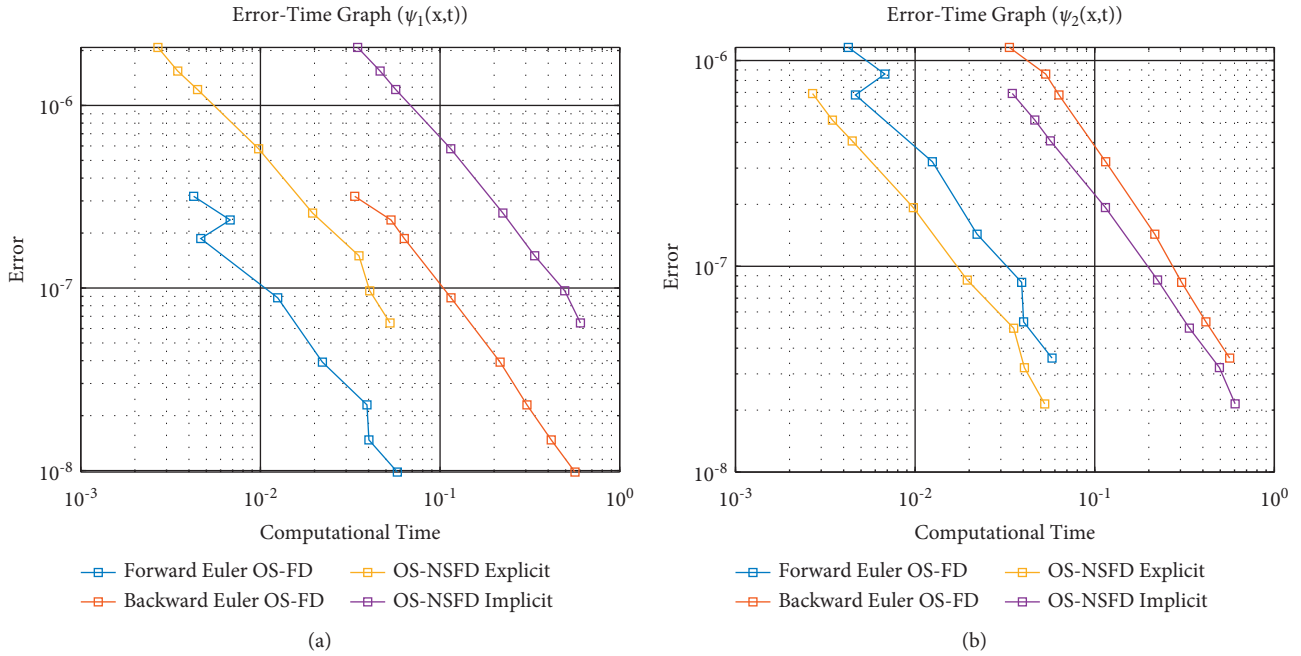
(a)

(b)

FIGURE 11: Log-log graphs. The error versus the computational time when solving the system subjected to the initial data. Three schemes are employed: forward Euler OS-FD technique, backward Euler OS-FD technique, OS-NSFD explicit technique, and OS-NSFD implicit technique. The graphs correspond to the solutions when the functions ψ_1 and ψ_2 of the Brusselator model are estimated. The parameters employed are $L = 1$, $T = 1$, $\vartheta_1 = 0.05$, $\vartheta_2 = 0.02$, $M = 100$, and $\varepsilon_{\psi_1} = \varepsilon_{\psi_1} = 10^{-4}$. The exact solution was approximated using $N = 20000$. (a) Error time graph for ψ_1. (b) Error time graph for ψ_2.
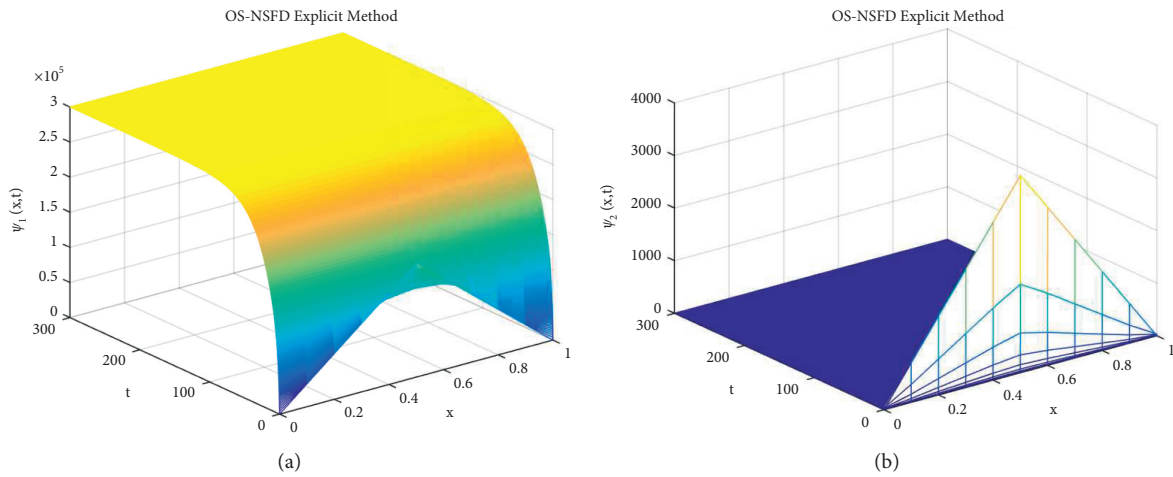

(a)

(b)

FIGURE 12: Solution graphs of ψ_1 and ψ_2 (susceptible and infected population densities) using the NSFD explicit splitting method at $\kappa = 0.1, \lambda_1 = \lambda_2 = 0.05$. (a) Solution graph of ψ_1. (b) Solution graph of ψ_2.

important features of reaction diffusion systems like as positivity, boundedness, and stability at equilibrium points.

6. Schnakenberg Model

Schnakenberg model is autocatalytic in nature given in 1979 [42]. The Schnakenberg model is a coupled reaction diffusion system [43] given as

$$\frac{\partial \psi_1}{\partial t} = \frac{\partial^2 \psi_1}{\partial x^2} + \vartheta_3 \left(\vartheta_1 - \psi_1 + (\psi_1)^2 \psi_2 \right), \quad (45)$$

$$\frac{\partial \psi_2}{\partial t} = \varepsilon_{\psi_2} \frac{\partial^2 \psi_2}{\partial x^2} + \vartheta_3 \left(\vartheta_2 - (\psi_1)^2 \psi_2 \right), \quad (46)$$
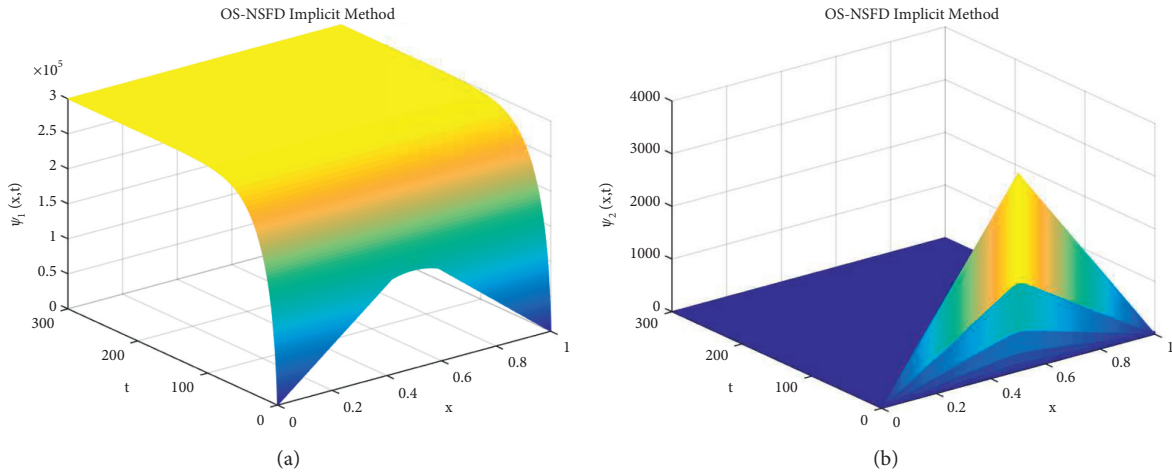
with initial conditions

FIGURE 13: Solution graphs of ψ_1 and ψ_2 (susceptible and infected population densities) using NSFD implicit splitting method at $\kappa = 0.002, \lambda_1 = \lambda_2 = 125$. (a) Solution graph of ψ_1. (b) Solution graph of ψ_2.
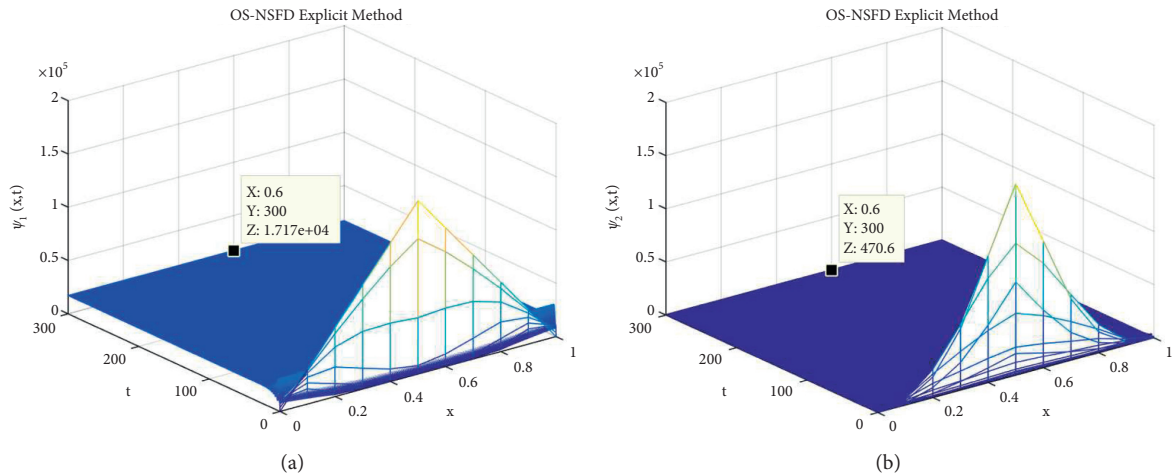

FIGURE 14: Solution graphs of ψ_1 and ψ_2 (susceptible and infected population densities) using the NSFD explicit splitting method at $\kappa = 0.1, \lambda_1 = \lambda_2 = 0.05$. (a) Solution graph of ψ_1. (b) Solution graph of ψ_2.
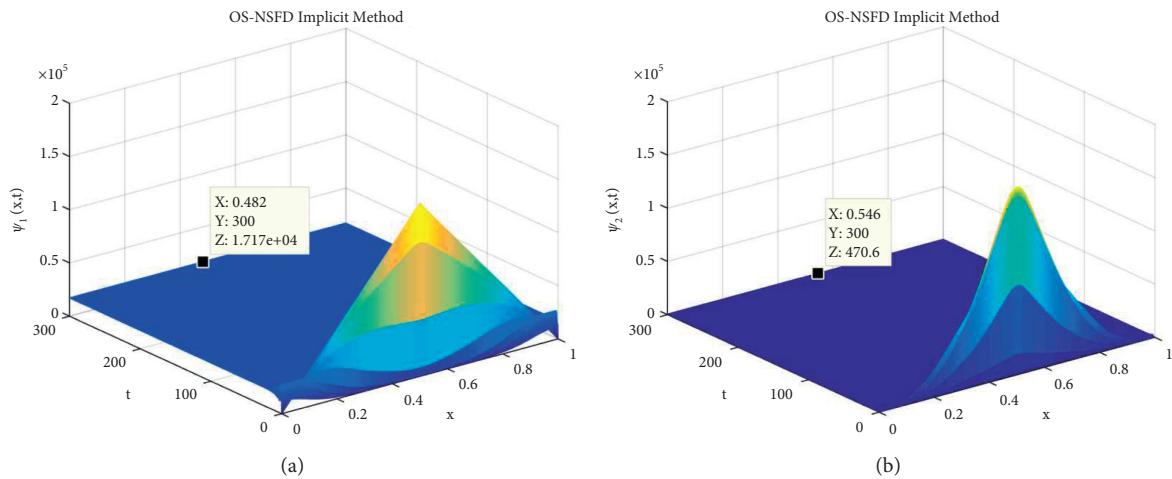

FIGURE 15: Solution graphs of ψ_1 and ψ_2 (susceptible and infected population densities) using the NSFD implicit splitting method at $\kappa = 0.002, \lambda_1 = \lambda_2 = 125$. (a) Solution graph of ψ_1. (b) Solution graph of ψ_2.
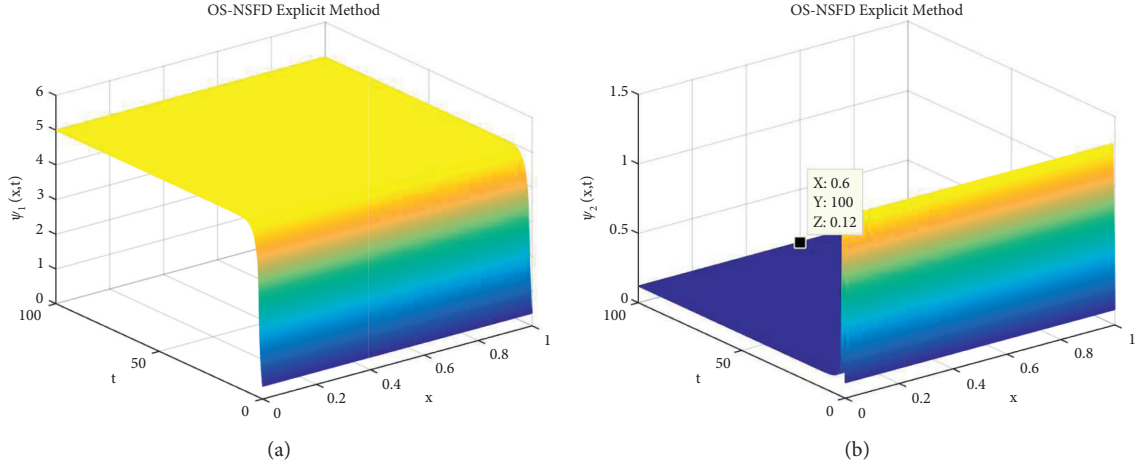
FIGURE 16: Mesh graphs of ψ_1 and ψ_2 (chemical concentration) using NSFD explicit splitting method at $\kappa = 0.1, \lambda_1 = 0.1, \lambda_2 = 0.00001$. (a) Mesh graph of ψ_1. (b) Mesh graph of ψ_2.
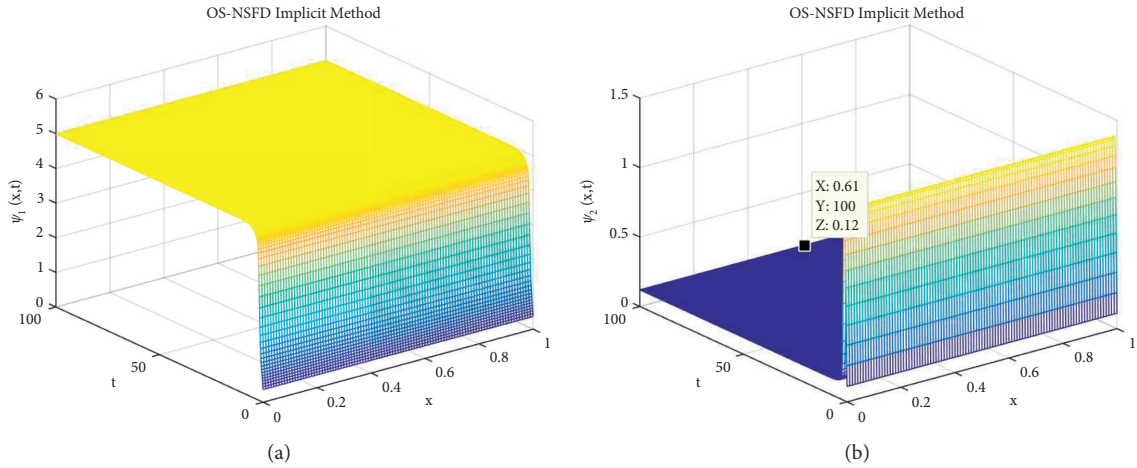

FIGURE 17: Mesh graphs of ψ_1 and ψ_2 (chemical concentration) using NSFD implicit splitting method at $\kappa = 0.01, \lambda_1 = 1000, \lambda_2 = 0.1$. (a) Mesh graph of ψ_1. (b) Mesh graph of ψ_2.

$$\psi_1(x, 0) = e^{-(1+0.001x)}, \tag{47}$$

$$\psi_2(x, 0) = \frac{1}{9}, \tag{48}$$

and no flux boundary conditions.

Here, ψ_1 and ψ_2 demonstrate the chemical concentrations of the two species. ϑ_1 and ϑ_2 are chemical kinetic positive constants, and ϑ_3 is the positive constant for the model which is dimensionless. The equilibrium point of systems (45) and (46) is (ψ_1^*, ψ_2^*), where $\psi_1^* = (\vartheta_1 + \vartheta_2)$ and $\psi_2^* = \vartheta_2/(\vartheta_1 + \vartheta_2)$. The equilibrium point is stable under the condition $\vartheta_2 - \vartheta_1 < (\vartheta_1 + \vartheta_2)^3$ [43]. If this condition violates, then the point (ψ_1^*, ψ_2^*) is unstable.

Now, we present the simulations of the above experiment. First, we take the values of parameters $\vartheta_1 = 2, \vartheta_2 = 3$, $\vartheta_3 = 0.5$, and $\varepsilon_{\psi_2} = 10^{-04}$ such that the condition $\vartheta_2 - \vartheta_1 < (\vartheta_1 + \vartheta_2)^3$ satisfies. For these numerical values, the equilibrium point is $(\psi_1^*, \psi_2^*) = (5, 0.12)$.

The graphs in Figures 16 and 17 show the consistent behavior of both OS-NSFD explicit and implicit schemes. Both schemes show that the graphs converge towards the point $(\psi_1^*, \psi_2^*) = (5, 0.12)$. We are not presenting the graphical solution with forward Euler and backward Euler splitting schemes, but it is confirmed that the schemes will present the inconsistent behavior for different values of parameters as shown earlier for the Brusselator model.

Now, we choose the values of parameters $\vartheta_1 = 0.1$, $\vartheta_2 = 0.4$, $\vartheta_3 = 0.5$, and $\varepsilon_{\psi_2} = 10^{-04}$ such that the condition $\vartheta_2 - \vartheta_1 < (\vartheta_1 + \vartheta_2)^3$ violates.

As we discussed earlier that systems (45) and (46) show the unstable behavior if the condition $\vartheta_2 - \vartheta_1 < (\vartheta_1 + \vartheta_2)^3$ does not satisfy. The graphs in Figures 18 and 19 clarify that OS-NSFD explicit and implicit schemes also reveal the unstable behavior which is possessed by the continuous system.

It is important to note that all the parameters and step sizes are kept same during the simulations. It is the stability
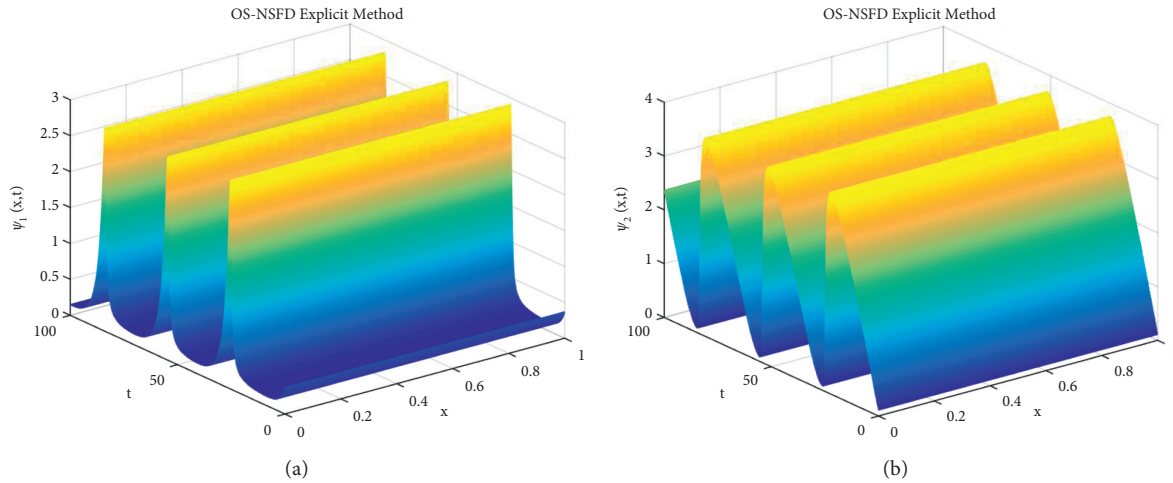
(a)

(b)

FIGURE 18: Mesh graphs of ψ_1 and ψ_2 (chemical concentration) using the NSFD explicit splitting method at $\kappa = 0.1, \lambda_1 = 0.1, \lambda_2 = 0.00001$. (a) Mesh graph of ψ_1. (b) Mesh graph of ψ_2.
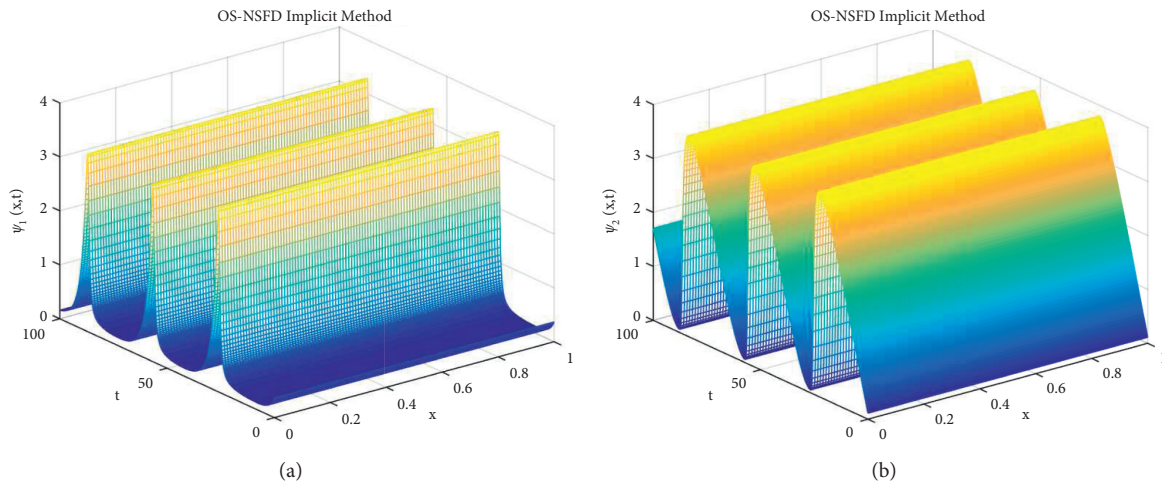

(a)

(b)

FIGURE 19: Mesh graphs of ψ_1 and ψ_2 (chemical concentration) using the NSFD implicit splitting method at $\kappa = 0.01, \lambda_1 = 1000, \lambda_2 = 0.1$. (a) Mesh graph of ψ_1. (b) Mesh graph of ψ_2.

condition that also plays an important role in describing the stability of the system.

7. Conclusion

In this article, four numerical schemes based on finite difference approximation are presented for solving different reaction-diffusion models in one-space dimension. It has been observed that two classical methods fail to provide accurate solution. Also, these schemes do not hold the positivity condition of the unknown variables in the continuous system. To overcome this issue, two new positivity preserving techniques have been proposed, based on OS-NSFD schemes. Our proposed methods not only provide the positive solution but also retain the essential physical attributes of the state variables. The designed schemes are applied on the Brusselator model, Schnakenberg model, and SIR epidemic model.

The simulations are carried out to obtain the graphical solutions. The numerical results ascertained that the newly designed NSFD splitting schemes have some prominent features of the solution such as positivity of the solutions and stability at equilibrium points of the continuous system. One of the main significance is that the designed schemes do not generate the contrived chaos.

The OS-NSFD methods grant the positive solution irrespective of the step sizes. So, these schemes are unconditionally positivity preserving. Also, these schemes are time efficient and consistent.

The successful implementation of NSFD splitting schemes on three different problems show that our proposed schemes are futuristic and these techniques can be applied on various physical reaction diffusion problem in the fields of physical science, engineering, fluid mechanics, economics, and many more.

Data Availability

No data were used to support this work.

Conflicts of Interest

The authors declare no conflicts of interest.

References

[1] Z. Korpinar, M. Inc, M. S. Alshomrani, and D. Baleanu, "The deterministic and stochastic solutions of the Schrodinger equation with time conformable derivative in birefrigent fibers," *AIMS Mathematics*, vol. 5, no. 3, pp. 2326–2345, 2020.

[2] M. Partohaghighi, M. Inc, M. Bayram, and D. Baleanu, "On numerical solution of the time fractional advection-diffusion equation involving atangana-baleanu-caputo derivative," *Open Physics*, vol. 17, no. 1, pp. 816–822, 2019.

[3] M. M. A. Khater, D.-C. Lu, R. A. M. Attia, and M. Inç, "Analytical and approximate solutions for complex nonlinear schrödinger equation via generalized auxiliary equation and numerical schemes," *Communications in Theoretical Physics*, vol. 71, no. 11, p. 1267, 2019.

[4] R. Lefever and G. Nicolis, "Chemical instabilities and sustained oscillations," *Journal of Theoretical Biology*, vol. 30, no. 2, pp. 267–284, 1971.

[5] I. Prigogine and G. Nicolis, "Self-organisation in nonequilibrium systems: towards a dynamics of complexity," *Bifurcation Analysis*, Springer, Netherlands, pp. 3–12, 1985.

[6] I. Prigogine and R. Lefever, "Symmetry breaking instabilities in dissipative systems. II," *The Journal of Chemical Physics*, vol. 48, no. 4, pp. 1695–1700, 1968.

[7] J. J. Tyson, "Some further studies of nonlinear oscillations in chemical systems," *The Journal of Chemical Physics*, AIP Publishing), vol. 58, no. 9, pp. 3919–3930, 1973.

[8] A. Turing, "The chemical basis of morphogenesis," *Bulletin of Mathematical Biology*, vol. 52, no. 1-2, pp. 153–197, 1990.

[9] S. Kumar, R. Jiwari, and R. C. Mittal, "Numerical simulation for computational modelling of reaction diffusion Brusselator model arising in chemical processes," *Journal of Mathematical Chemistry*, Springer Science and Business Media, vol. 57, , pp. 149–179, 2019.

[10] R. C. Mittal and R. Rohila, "A study of one dimensional nonlinear diffusion equations by Bernstein polynomial based differential quadrature method," *Journal of Mathematical Chemistry*, vol. 55, no. 2, pp. 673–695, 2016.

[11] R. C. Mittal and R. Rohila, "Numerical simulation of reaction-diffusion systems by modified cubic B-spline differential quadrature method," *Chaos, Solitons & Fractals*, vol. 92, pp. 9–19, 2016.

[12] S. Siraj-ul-Islam, A. Ali, and S. Haq, "A computational modeling of the behavior of the two-dimensional reaction-diffusion Brusselator system," *Applied Mathematical Modelling*, vol. 34, no. 12, pp. 3896–3909, 2010.

[13] R. Jiwari and J. Yuan, "A computational modeling of two dimensional reaction-diffusion Brusselator system arising in chemical processes," *Journal of Mathematical Chemistry*, Springer Science and Business Media, vol. 52, no. 6, pp. 1535–1551, 2014.

[14] S. Dahiya and R. C. Mittal, "A modified cubic B-spline differential quadrature method for three-dimensional non-linear diffusion equations," *Open Physics*, vol. 15, no. 1, pp. 453–463, 2017.

[15] Z. Lin, R. Ruiz-Baier, and C. Tian, "Finite volume element approximation of an inhomogeneous Brusselator model with cross-diffusion," *Journal of Computational Physics*, vol. 256, pp. 806–823, 2014.

[16] F. Khani, F. Samadi, and S. Hamedi-Nezhad, "New exact solutions of the brusselator reaction diffusion model using the exp-function method," *Mathematical Problems in Engineering*, vol. 2009, pp. 1–9, 2009.

[17] R. C. Mittal and R. Jiwari, "Numerical solution of two-dimensional reaction-diffusion Brusselator system," *Applied Mathematics and Computation*, vol. 217, no. 12, pp. 5404–5415, 2011.

[18] H. y. Alfifi, "Semi-analytical solutions for the brusselator reaction-diffusion model," *ANZIAM Journal*, vol. 59, no. 2, pp. 167–182, 2017.

[19] S. Alkhalaf, "Third-order approximate solution of chemical reaction-diffusion brusselator system using optimal homotopy asymptotic method," *Advances in Mathematical Physics*, vol. 2017, pp. 1–8, 2017.

[20] M. Ghergu and V. Rădulescu, "Turing patterns in general reaction-diffusion systems of brusselator type," *Communications in Contemporary Mathematics*, vol. 12, no. 4, pp. 661–679, 2010.

[21] Z. U. A. Zafar, K. Rehan, M. Mushtaq, and M. Rafiq, "Numerical treatment for nonlinear Brusselator chemical model," *Journal of Difference Equations and Applications*, vol. 23, no. 3, pp. 521–538, 2016.

[22] M. A. Zaky and A. S. Hendy, "An efficient dissipation-preserving Legendre-Galerkin spectral method for the Higgs boson equation in the de Sitter spacetime universe," *Applied Numerical Mathematics*, vol. 160, pp. 281–295, 2021.

[23] M. Abbaszadeh, M. Dehghan, M. A. Zaky, and A. S. Hendy, "Interpolating stabilized element free galerkin method for neutral delay fractional damped diffusion-wave equation," *Journal of Function Spaces*, vol. 2021, Article ID 6665420, 11 pages, 2021.

[24] A. K. Omran, M. A. Zaky, A. S. Hendy, and V. G. Pimenov, "An efficient hybrid numerical scheme for nonlinear multi-term caputo time and riesz space fractional-order diffusion equations with delay," *Journal of Function Spaces*, vol. 2021, Article ID 5922853, , 2021.

[25] A. S. Hendy, M. A. Zaky, and M. Abbaszadeh, "Long time behavior of Robin boundary sub-diffusion equation with fractional partial derivatives of Caputo type in differential and difference settings," *Mathematics and Computers in Simulation*, vol. 190, pp. 1370–1378, 2021.

[26] S. Nandal, M. A. Zaky, and R. H. De Staeien, "Numerical simulation for a multidimensional fourth-order nonlinear fractional subdiffusion model with time delay," *Mathematics*, vol. 9, no. 23, p. 3050, 2021.

[27] A. S. Hendy, M. A. Zaky, R. M. Hafeez, and R. H. De Staeien, "The impact of memory effect on space fractional strong quantum couplers with tunable decay behavior and its numerical simulation," *Scientific Reports*, vol. 11, no. 1, pp. 1–15, 2021.

[28] H. Selvitopi, M. A. Zaky, and A. S. Hendy, "Crank-Nicolson/finite element approximation for the Schrödinger equation in the de Sitter spacetime," *Physica Scripta*, vol. 96, no. 12, Article ID 124010, 2021.

[29] R. E. Mickens, *Nonstandard Finite Difference Models of Differential Equations*, World Scientific, Singapore, 1993.

[30] N. Ahmed, T. S.S., M. Rafiq, M. A. Rehman, M. Ali, and M. O. Ahmad, "Positivity preserving operator splitting nonstandard finite difference methods for SEIR reaction

diffusion model," *Open Mathematics*, vol. 17, no. 1, pp. 313–330, 2019.

[31] M. Zhang and Q. Zhang, "A positivity preserving numerical method for stochastic R&D model," *Applied Mathematics and Computation*, vol. 351, pp. 193–203, 2019.

[32] N. Ahmed, M. Rafiq, M. A. Rehman, M. S. Iqbal, and M. Ali, "Numerical modeling of three dimensional Brusselator reaction diffusion system," *AIP Advances*, vol. 9, no. 1, Article ID 015205, 2019.

[33] J. Tan, H. Yang, W. Men, and Y. Guo, "Construction of positivity preserving numerical method for jump-diffusion option pricing models," *Journal of Computational and Applied Mathematics*, vol. 320, pp. 96–100, 2017.

[34] N. Ahmed, Z. Wei, D. Baleanu, M. Rafiq, and M. A. Rehman, "Spatio-temporal numerical modeling of reaction-diffusion measles epidemic system," *Chaos: An Interdisciplinary Journal of Nonlinear Science*, vol. 29, no. 10, Article ID 103101, 2019.

[35] N. Ahmed, M. Jawaz, M. Rafiq, M. A. Rehman, M. Ali, and M. O. Ahmad, "Numerical treatment of an epidemic model with spatial diffusion," *Journal of Applied Environmental and Biological Sciences*, vol. 8, no. 6, pp. 17–29, 2018.

[36] N. Ahmed, M. Rafiq, M. A. Rehman, M. Ali, and M. O. Ahmad, "Numerical modeling of SEIR measles dynamics with diffusion," *Communications in Mathematics and Applications*, vol. 9, pp. 315–326, 2018.

[37] N. Ahmed, N. Shahid, Z. Iqbal et al., "Numerical modeling of SEIQV epidemic model with saturated incidence rate," *Journal of Applied Environmental and Biological Sciences*, vol. 8, 2018.

[38] R. C. Harwood, *Operator Splitting Method and Applications for Semilinear Parabolic Partial Differential Equations*, George Fox University, USA, 2011.

[39] R. C. Harwood, V. S. Manoranjan, and D. B. Edwards, "Lead-acid battery model under discharge with a fast splitting method," *IEEE Transactions on Energy Conversion*, vol. 26, no. 4, pp. 1109–1117, 2011.

[40] T. Fujimoto and R. Ranade, "Two characterizations of inverse-positive matrices: the Hawkins-Simon condition and the Le Chatelier-Braun principle," *The Electronic Journal of Linear Algebra*, vol. 11, no. 1, 2004.

[41] S. Chinviriyasit and W. Chinviriyasit, "Numerical modelling of an SIR epidemic model with diffusion," *Applied Mathematics and Computation*, vol. 216, no. 2, pp. 395–409, 2010.

[42] J. Schnakenberg, "Simple chemical reaction systems with limit cycle behaviour," *Journal of Theoretical Biology*, vol. 81, pp. 389–400, 1979.

[43] Z. Hammouch, T. Mekkaoui, and F. B. M. Belgacem, "Numerical simulations for a variable order fractional Schnakenberg model," *AIP Conference Proceedings*, vol. 1637, 2014.